



# Preparation of TiO<sub>2</sub> Sols with High Solid Contents by Sol Gel Method

Ming-Hsien Lu, Yu-Wen Chen\*

Department of Chemical and Materials Engineering, National Central University, Jhong-Li, Taiwan

## Email address:

ywchen@cc.ncu.edu.tw (Yu-Wen Chen)

\*Corresponding author

## To cite this article:

Ming-Hsien Lu, Yu-Wen Chen. Preparation of TiO<sub>2</sub> Sols with High Solid Contents by Sol Gel Method. *International Journal of Biochemistry, Biophysics & Molecular Biology*. Vol. 6, No. 2, 2021, pp. 26-33. doi: 10.11648/j.ijbbmb.20210602.11

Received: June 16, 2021; Accepted: July 14, 2021; Published: July 22, 2021

**Abstract:** Titanium oxide has been extensively used as a photocatalytic material because of its excellent UV light-responsive effect, high refractive index, and high chemical stability. TiO<sub>2</sub> in anatase phase for applications in optical or electronic devices and photocatalysis has generally been used in the form of a thin film. The aim of this study was to prepare a stable TiO<sub>2</sub> sol with high solid content. Therefore one can use less coating time to have a mono layer of TiO<sub>2</sub> film on the substrate. In this study, TiCl<sub>4</sub> was slowly added to the distilled water in an ice bath. Aqueous solution of sodium hydroxide was added to adjust the pH of the solution to between 8 and 12 to form titanium hydroxide gel. After aging for a period of time, the Ti(OH)<sub>4</sub> gel was filtered and sufficiently washed. The filtered cake was repulped in water. Hydrochloric acid, as a catalyst for polycondensation, was slowly added to the solution with stirring. After poly-condensation reaction and crystallization, a transparent suspended TiO<sub>2</sub> sol was formed. XRD results show that the crystalline phase was anatase. The suspended TiO<sub>2</sub> particles were rhombus primary particles with the major axis ca. 20 nm and the minor axis ca. 5 nm. The sample prepared at pH 8 had the largest BET surface area of 141 cm<sup>3</sup>/g among all samples. The best preparation condition to have the smallest TiO<sub>2</sub> particles are Ti: H = 1: 1 (atomic ratio), 10% solid content of TiO<sub>2</sub>, and hydroxypropyl cellulose with viscosity of 150-400 cps as a surfactant. The thin film was obtained by dip-coating the glass in TiO<sub>2</sub> sol. Since the sol had high solid content, the coating time became less. The dip-coating on glass was less than three times to have one monolayer TiO<sub>2</sub>. The transparent TiO<sub>2</sub> thin film had super-hydrophilicity after illumination by UV light.

**Keywords:** Titania, Photocatalysis, Sol-gel, Coating, Anatase

## 1. Introduction

Titanium dioxide has been used in a wide range of applications. [1-12] It is low cost, chemically stable, non-toxic and bio-compatible. Titania has been used as a photocatalyst, implant material in dental, orthopedic and osteosynthesis applications. TiO<sub>2</sub> thin films have a high refractive index that makes TiO<sub>2</sub> suitable for optical applications. TiO<sub>2</sub> is widely used for photocatalysis to destruct dyes, pollutant, and bacteria under UV light illumination.

TiO<sub>2</sub> sol has been used to prepare TiO<sub>2</sub> film on substrates by various coating techniques.[1-23] Various preparation methods to prepare TiO<sub>2</sub> sols have been reported in the literature. [5-9, 19-21] Most of researchers used titanium alkoxide as the precursor. [2-4, 14, 25] However, titanium alkoxide is expensive and not stable in air. Some researchers

used TiCl<sub>4</sub> as the precursor. [14, 15] However, most of sols have low solid content. [22-31] It would need many times coating to have one monolayer TiO<sub>2</sub> thin film.

The aim of this study was to develop a method to prepare TiO<sub>2</sub> sol which has high solid content. In this study, TiCl<sub>4</sub> was used as the starting material. It was converted to Ti(OH)<sub>4</sub> gel with NaOH. The gel was then converted to TiO<sub>2</sub> sol by adding HCl as the catalyst for polycondensation and crystallization. In this study, with carefully control pH value and amount of NaOH and HCl, we have successfully prepare TiO<sub>2</sub> sol with 10% solid content.

## 2. Experimental

### 2.1. Chemicals

Titanium tetrachloride (> 99.9%), sodium hydroxide

(>96%), and hydrochloric acid (35%) were from Showa Chemicals Co. Two types of hydroxypropyl cellulose (HPC, viscosity = 6-10 cps and 150-400 cps, 2% in water at 20°C) were from Merck.

## 2.2. Synthesis of TiO<sub>2</sub> Sol

TiCl<sub>4</sub> was used as a precursor. It was slowly added to the distilled water in an ice bath at 5°C. When TiCl<sub>4</sub> dissolved in distilled water, the heat of the exothermic reaction explosively generated the formation of orthotitanic acid. Ti(OH)<sub>4</sub>. Because the formation of this species disturbed homogeneous precipitation, 5 ml of hydrochloric acid (35% HCl) per 100 ml of distilled water was added to prevent formation of orthotitanic acid. Aqueous solution of sodium hydroxide solution was slowly added to adjust the pH of the system to 8-12. After aging for a period of time, the peptizate sol was filtered and sufficiently washed to remove chlorine ion from the cake. The cake was repulped in water. Hydrochloric acid was slowly added to the solution with stirring. After condensation reaction and crystallization, the transparent suspended TiO<sub>2</sub> sol was obtained.

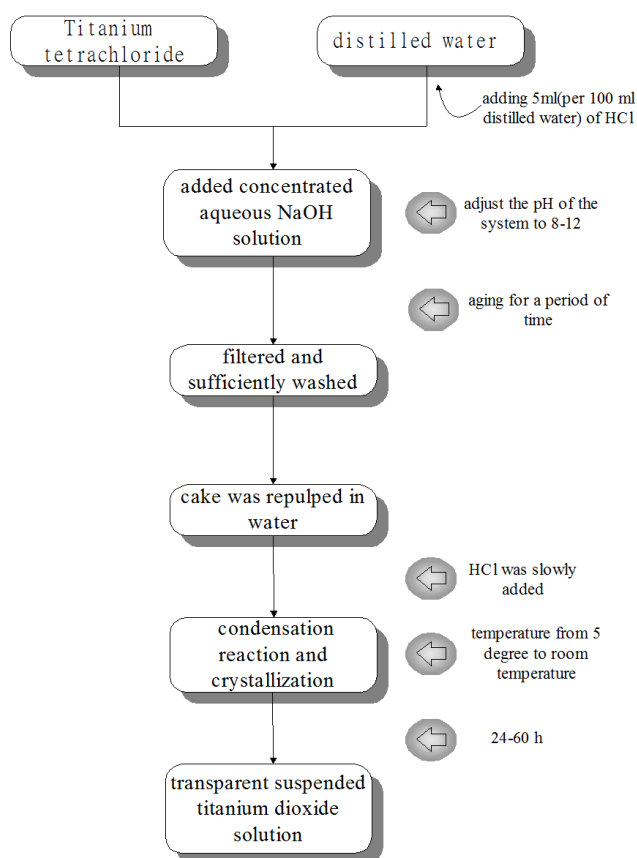


Figure 1. Preparation method of transparent suspended TiO<sub>2</sub> sol.

## 2.3. Characterization

### 2.3.1. X-ray Diffraction (XRD)

The crystalline structures of the products were analyzed by X-ray powder diffraction using a Siemens D500 automatic powder diffractometer system. Nickel-filtered Cu K<sub>α</sub> radiation

( $\lambda = 0.15418$  nm) was used with a generator voltage of 40 kV and a current of 29 mA. The Bragg-Brentano focusing geometry was employed with an automatic divergence slit (irradiated sample length was 12.5 mm), a receiving slit of 0.1 mm, a fixed slit of 4° and a proportional counter as a detector. It was operated in the step scan mode, at scanning speeds of 0.05° 2 $\theta$ /s and 1 second step time from the range 20° to 80°. Scherrer's equation was used to calculate the crystallite size of TiO<sub>2</sub> crystal:

$$D = \frac{k\lambda}{\beta \cos \theta} \quad (1)$$

where D is crystallite particle size,  $\kappa$  is a constant of 0.94,  $\lambda$  is X-ray wavelength (0.154 nm),  $\beta$  is half maximum line breadth, and  $\theta$  is Bragg angle.

### 2.3.2. N<sub>2</sub> Sorption

The measurement of the surface areas of the samples were achieved by Brunauer-Emmett-Teller (BET) method, and the pore size distributions were determined by Barrett-Joyner-Halenda (BJH) method. The N<sub>2</sub> sorption was carried out in a ASAP 2100 instrument (Micromeritics Co.).

### 2.3.3. Thermogravimetric Analysis (TGA)

The TGA was carried out at a Perkin Elmer TGA-7 with a heating rate from 50 to 600°C. Those samples were heated in nitrogen at a heating rate of 10°C /min.

### 2.3.4. Differential Scanning Calorimetry (DSC)

DSC analysis was measure by using Perkin Elmer DSC-7 with a heating rate of 10°C /min from 50 to 450°C.

### 2.3.5. Scanning Electron Microscopy (SEM)

Sample was dried at 35°C, then placed on a stage for SEM. The sample was coated with Au for 4 min before the experiment and was observed using a Hitachi S-800. It was operated at 200 kV.

### 2.3.6. Transmission Electron Microscopy (TEM)

The suspended TiO<sub>2</sub> was deposited on a grid with a holey carbon copper film and placed several days at room temperature. It was observed in a JEM-1200 EX II electron microscope operating at 160 kV. The magnification was calibrated in pixel/nm on the camera.

### 2.3.7. Dynamic Light Scattering (DLS)

The particle size of the sample was measured by DLS using Zetasizer 3000. Dynamic light scattering measures Brownian motion and relates it to size. Random movement of particles due to bombardment by the solvent molecules that surround them, and the larger the particle is, the slower the Brownian motion is. One can calculate the hydrodynamic diameter d(H) by using the Stokes-Einstein equation:

$$d(H) = \frac{\kappa\lambda}{3\pi\eta D} \quad (2)$$

where d(H) is hydrodynamic diameter,  $\kappa$  is Boltzmann's

constant,  $T$  is absolute temperature,  $\eta$  is viscosity, and  $D$  is diffusion coefficient.

### 2.3.8. Ultraviolet/Visible Absorption (UV-vis)

The diffuse reflectance UV-vis absorption measurement was carried out with a Jasco UV V-500 spectrophotometer. The sample was loaded in a quartz cell with suprasil windows, and spectra were collected in the range from 300 nm to 800 nm against quartz standard.

### 2.3.9. Contact Angle Meter

The contact angle analysis was measure by using Model CA-D (Kyowa Interface Science Co., Ltd. Japan). Glass slide was used as a substrate.  $\text{TiO}_2$  was coated on the glass substrate several times, then small amount of deionized water was drop on it. The contact angle is based on the equation as follow:

$$\gamma = \frac{r h \rho g}{2 \cos \theta} \quad (3)$$

where  $\gamma$  is surface tension of a capillary,  $r$  is radius of a capillary,  $h$  is the height of liquid,  $\rho$  is the density of liquid,  $g$  is gravity, and  $\theta$  is contact angle.

## 3. Results and Discussion

This research was devoted to prepare a stable and suspended  $\text{TiO}_2$  sol with high solid content, small particles size, and anatase crystalline phase. Five preparation parameters were studied, i.e., pH value,  $[\text{H}^+]/[\text{Ti}]$  ratio, HCl concentration, stored temperature, and surfactant.

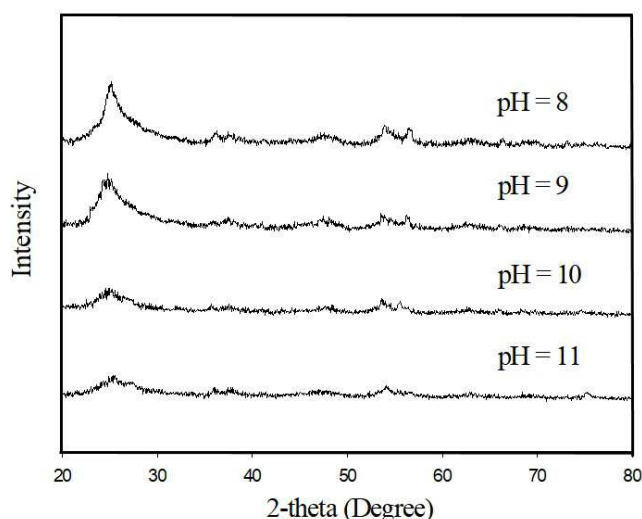


Figure 2. XRD patterns of  $\text{TiO}_2$  prepared at different pH values.

### 3.1. Particle Size Distribution

#### Effects of pH value

After dissolving  $\text{TiCl}_4$  in water, NaOH was added to adjust the pH value of the solution. Based on the literature [32] the isoelectric point (IEP) of  $\text{TiO}_2$  is at pH 4.5-6.8. If the pH value is adjusted to this region, there is no repulsive force between particles so as to maintain the dispersion of the particles. The

particles collide in each other, and the particles will aggregate and precipitate due to vander Waals interaction. Due to the drawback described above, the pH value was adjusted to greater than 8 or to value lower than 3 to have stable  $\text{TiO}_2$  suspension.

As the  $\text{TiO}_2$  particle was small, the XRD peak should appear, but not intense. As shown in Figure 2, all the samples showed anatase XRD peaks with low intensity. The stable anatase  $\text{TiO}_2$  was obtained at pH 8-11. The samples prepared at pH 8 and 9 had more intense XRD peaks than those prepared at pH 10 and 11. It should be noted that there was only one major peak in the XRD patterns. It indicates the formation of anatase, but the crystallite size is small. Scherrer's equation was used to calculate the mean diameter of the crystallites. The sample prepared at pH 8 had the smallest crystallites among all samples (Table 1).

Table 1. Mean diameters of  $\text{TiO}_2$  crystallites prepared at various pH values (Mean diameter was calculated from XRD result).

| pH value                             | 8   | 9   | 10  | 11  | 12  |
|--------------------------------------|-----|-----|-----|-----|-----|
| Mean diameter (nm) of $\text{TiO}_2$ | 7.8 | 7.9 | 8.1 | 8.3 | 8.7 |

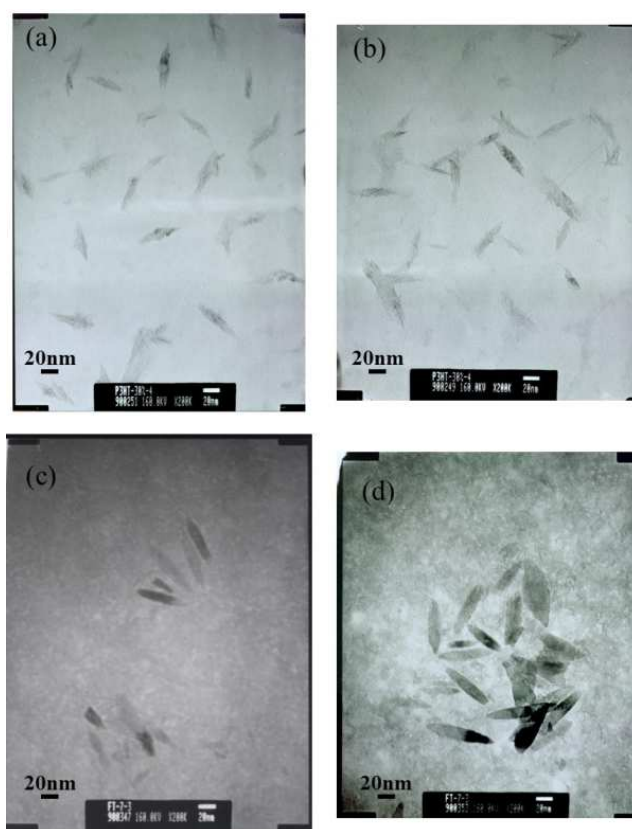


Figure 3. TEM image of  $\text{TiO}_2$  prepared at different pH values. (a) pH = 8; (b) pH = 9; (c) pH = 10; (d) pH = 11 (store temperature = 30°C).

Figure 3 shows the TEM images of the samples prepared at various pH values. The samples prepared pH 8 and 9 had small particle sizes than those prepared at pH 10 and 11. As shown in the TEM images (Figure 3), the primary particles of the sample prepared at pH 8 were rhombus shape with major axis of 20 nm and minor axis of 5 nm. At pH 11 and 12, the major axis of the rhombus form was 40-50 nm and the minor

axis was 10 nm. One can conclude that at pH of 8, well-crystallized anatase TiO<sub>2</sub> particles with nano size was obtained. The DLS results show that the particles distributed in 5-10 nm size were 92%, and only 8% of particles aggregated into secondary particles. One can obtain the particles size from XRD, TEM and DLS. The particle sizes of TiO<sub>2</sub> from these three methods are listed in Table 2. It shows that the particle sizes measured from 3 methods are consistent. All of the results show that the particle of TiO<sub>2</sub> were in nano size.

**Table 2.** The particles size distribution of TiO<sub>2</sub>.

| Instrument         | XRD    | TEM                                       | DLS                               |
|--------------------|--------|---|-----------------------------------|
| Mean diameter (nm) | 7.8 nm | Major axis of 20 nm<br>Minor axis of 5 nm | Main in 5-10 nm<br>Minor in 30 nm |

Table 3 shows the effect of calcinations temperature on the pore structure of TiO<sub>2</sub> powder. The sample calcined at 200°C had the highest BET surface area among all samples. The average pore diameter increased with an increase of calcinations temperature.

**Table 3.** Surface area and pore structure of the sample from N<sub>2</sub> sorption.

| Sample               | BET surface area (m <sup>2</sup> /g) | BJH pore volume (cm <sup>3</sup> /g) | BJH pore diameter (Å) | H-K Pore diameter (Å) |
|----------------------|--------------------------------------|--------------------------------------|-----------------------|-----------------------|
| pH= 8 dried at 80 °C | 141                                  | 0.13                                 | 8.9                   | 5.1                   |
| Calcined at 100°C    | 187                                  | 0.15                                 | 12.7                  | 5.4                   |
| Calcined at 200°C    | 191                                  | 0.15                                 | 15.1                  | 5.6                   |
| Calcined at 300°C    | 109                                  | 0.10                                 | 25.3                  | 6.1                   |

### 3.2. Effects of [H<sup>+</sup>]/[Ti] Ratio

In general, while using inorganic salt to produce TiO<sub>2</sub>, most researchers used strong acid, such as HNO<sub>3</sub> or HCl, as a catalyst to promote poly-condensation reaction of the gel, and the molar ratio of [H<sup>+</sup>]/[Ti] was ~1. In this study, [H<sup>+</sup>]/[Ti] ratios of 0.6, 0.8, 1, and 1.5, respectively, were used to investigate the effect of [H<sup>+</sup>]/[Ti] ratio on the morphology of TiO<sub>2</sub>. When [H<sup>+</sup>]/[Ti] ratio was at about 0.6 and 0.8, longer time was needed to undergo condensation reaction and crystal growth, the TiO<sub>2</sub> was not well-crystallized and the sol was not transparent. There was some non-dissociate orthotitanic acid that formed TiO<sub>2</sub>. At [H<sup>+</sup>]/[Ti] ratio of 1 and 1.5, the effects of acid amount on condensation reaction and crystal growth time were observed. As [H<sup>+</sup>]/[Ti] ratio of 1.5, the time needed for condensation reaction and crystal growth was about 24 h, while at [H<sup>+</sup>]/[Ti] ratio of 1, the time needed was 48 h. As shown in Figure 5, the difference in the crystallinities of the samples at [H<sup>+</sup>]/[Ti] ratio between 1.5 and 1 was lower than those of 1 and 0.6, 0.8. It should be noted that the intense XRD peak means large crystallite size. The objective of this study was to synthesize small crystals. In other word, the XRD peaks should be detectable and not intense.

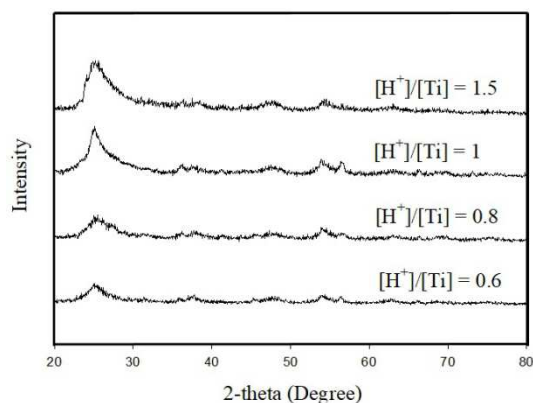


**Figure 4.** XRD patterns of TiO<sub>2</sub> prepared at different [H<sup>+</sup>]/[Ti] ratios.

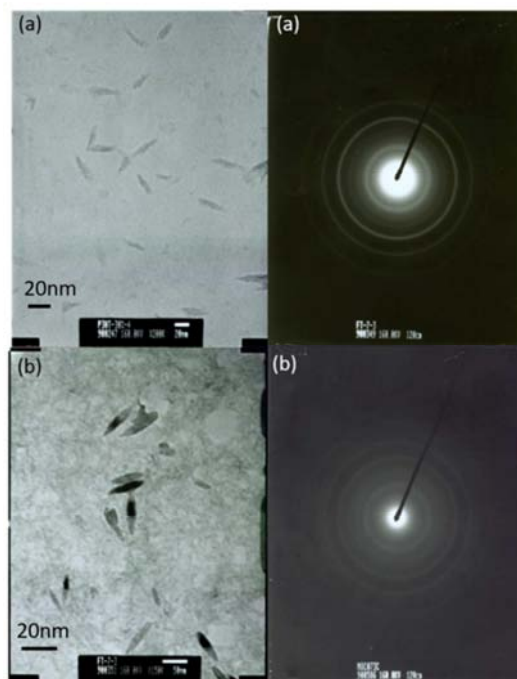


**Figure 5.** TEM image of TiO<sub>2</sub> prepared at pH=8 and (a) [H<sup>+</sup>]/[Ti] = 1, and (b) TEM image of TiO<sub>2</sub> prepared at pH=8 and [H<sup>+</sup>]/[Ti] = 1.5.

### 3.3. Effects of HCl Concentration

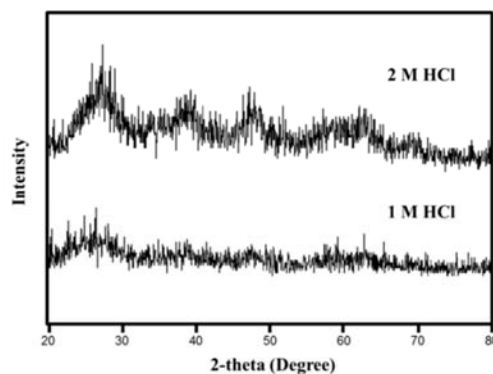


**Figure 6.** XRD patterns of TiO<sub>2</sub> prepared at different concentrations of HCl (pH =9; [H<sup>+</sup>]/[Ti] = 1).



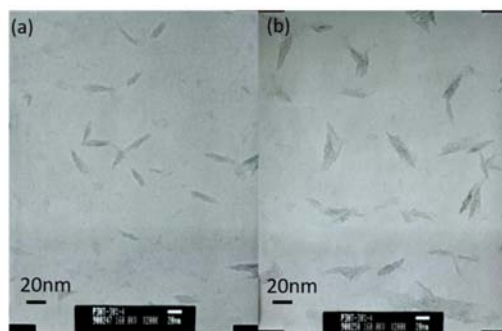


**Figure 7.** TEM image of  $\text{TiO}_2$  prepared at different HCl concentration. (a) pH=8, 1M HCl; (b) pH=8, 2M HCl.

From XRD patterns (Figure 6), one can see that the crystallinity of the sample prepared by 2 M HCl was higher than that prepared by 1 M HCl. Besides, the time needed for condensation reaction and crystal growth by 2 M HCl was 36 h, which was shorter than that needed for the sample prepared by 1 M HCl. Figure 7 shows the TEM images of the samples prepared by 1 M HCl and 2 M HCl. It clearly shows that the sample prepared by 1 M HCl was smaller than that by 2 M HCl. Based on the above results, one can conclude that the compositions of acid, Ti, and water could affect the formation of  $\text{TiO}_2$  nanocrystal. The higher the concentration of acid is, the higher the ratio of  $[\text{H}^+]/[\text{Ti}]$  ratio is, and the shorter the time is needed for condensation reaction and crystal growth. The best crystallized nano-sized  $\text{TiO}_2$  was obtained from the short time of crystallization, strong acid, high  $[\text{H}^+]/[\text{Ti}]$  ratio. The zeta potential would change and affected the preservation of the suspension. This will be discussed in latter section. If the crystalline particles with small diameter and high crystallinity is needed, one can immediately add basic solution (such as  $\text{NH}_4\text{OH}$  or  $\text{NaOH}$  aqueous solution) after condensation reaction and crystal growth to change the original pH range of acidic  $\text{TiO}_2$  crystal particles suspension solution to their isoelectric point. After precipitation,  $\text{TiO}_2$  particles become smaller, and its crystallinity is still high.

### 3.4. Effects of Stored Temperature on Particle Diameter

In this study, the temperature of preparation system was maintained at  $5^\circ\text{C}$ . After pH adjustment and aging, smaller orthotitanic acid particle could undergo condensation reaction and crystal growth, resulting in small diameter of  $\text{TiO}_2$  particle. Besides, in filtering and washing steps, the diameter of orthotitanic acid decreased with the number of filtering and washing times, especially when  $5^\circ\text{C}$  distilled water was used in washing.

The as-synthesized  $\text{TiO}_2$  sol was divided into two parts, one was stored at  $30^\circ\text{C}$  and the other at  $5^\circ\text{C}$ . TEM images (Figure 8) show that only a small part of the primary particles sample at  $5^\circ\text{C}$  aggregated to secondary particles and/or tertiary particles, especially the sol with high  $\text{TiO}_2$  solid content. This was due to smaller kinetic energy of particles at low temperature, resulting in fewer collisions, hence double layer (Stern layer and diffuse layer) was larger than van der Waals

force between particles, and stable suspension was obtained.

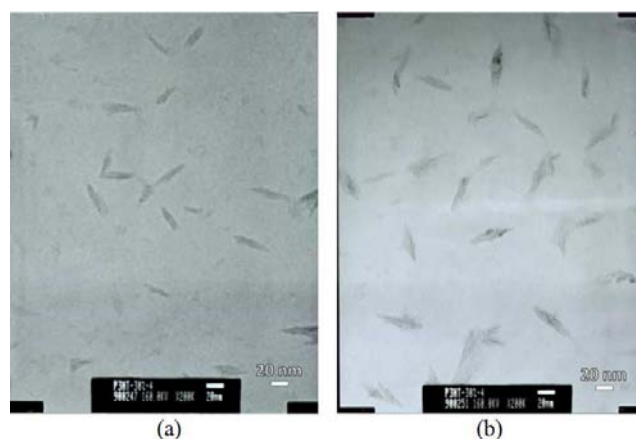


**Figure 8.** TEM image of  $\text{TiO}_2$  at different stored temperatures, (a) pH=8,  $5^\circ\text{C}$ ; (b) pH=8,  $30^\circ\text{C}$ .

### 3.5. Effects of HPC Surfactant

Many researchers [33] reported that adding surfactant could maintain stable suspension of particles. The surfactants play steric dispersing agent roles, which can keep particles in small diameters. [33] The surfactant can adsorb on  $\text{TiO}_2$  surface, change its zeta potential to provide stability of the sol, and avoid the aggregation of particles. Two kinds of HPC were used as surfactants in this study, one with viscosity of 6-10 cps, and the other with viscosity of 150-400 cps. They were added to  $\text{TiO}_2$  sol, respectively, to examine their effects on particle dispersion. After  $\text{TiO}_2$  sol was formed, 0.005 g/ml HPC was added to suspended  $\text{TiO}_2$  sol to disperse particle. It is found that the HPC with viscosity of 150-400 cps was better than that of HPC with viscosity of 6-10 cps. For the sample of  $\text{TiO}_2$  sol with solid content greater than 7%, HPC with viscosity of 150-400 cps was added to increase its stored time (Figure 9). Table 4 shows that adding HPC raised the suspension stability of 7%  $\text{TiO}_2$ , and the stored time for the sample with 10% solid content increased from 14 h to 30 h. This confirms that HPC changed the zeta potential of  $\text{TiO}_2$  particle and increased its suspension stability (Table 4).

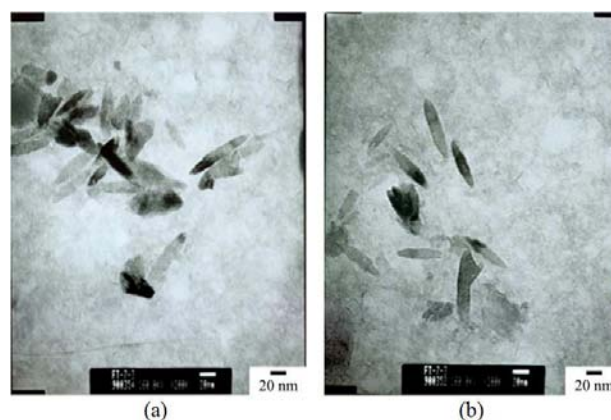


**Figure 9.** TEM image of  $\text{TiO}_2$  with various solid contents by adding HPC surfactant. (a) 10%; (b) 7%.

Table 4. Effects of surfactant.

|                     | 2.5% TiO <sub>2</sub>          | 5% TiO <sub>2</sub>            | 7% TiO <sub>2</sub>                         | 10% TiO <sub>2</sub> <sup>#</sup> |
|---------------------|--------------------------------|--------------------------------|---|-----------------------------------|
| Stored temp. (30°C) | Stable suspension for 3 months | Stable suspension for 3 months | Stable suspension for 14 h                  | Stable suspension for 13 h        |
| Stored temp. (5°C)  | Stable suspension for 3 months | Stable suspension for 3 months | Stable suspension for 26 h                  | Stable suspension for 14 h        |
| Adding HPC (30°C)   | Stable suspension for 3 months | Stable suspension for 3 months | Stable suspension with a little white color | Stable suspension for 26 h        |
| Adding HPC (5°C)    | Stable suspension for 3 months | Stable suspension for 3 months | Stable suspension with a little white color | Stable suspension for 30 h        |

### 3.6. UV-vis

The samples prepared in this study showed strong UV-vis absorption bands at 361 nm (Figure 10).

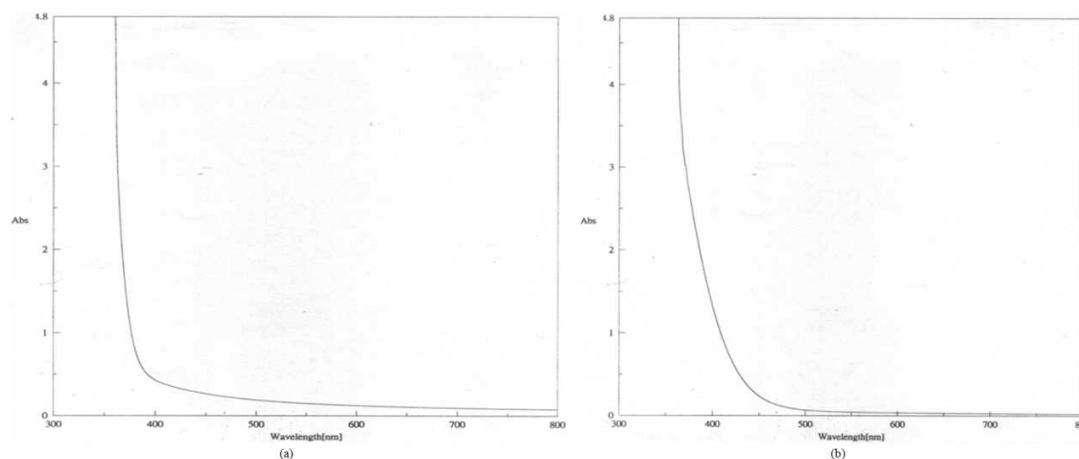


Figure 10. UV-visible spectra, (a) TiO<sub>2</sub> (dried at 80 °C), (b) TiO<sub>2</sub> calcined at 150 °C.

### Contact angle

TiO<sub>2</sub> was coated on glass substrate once or several times, then 40  $\mu$ l or 140  $\mu$ l deionized water was dropped on it. The results of contact angle show that if the glass was not washed thoroughly, it had dirt or oil substances, which would cause large degree of the contact angle. The clean glass without TiO<sub>2</sub> film attracted water molecules with its 'OH radicals on slide glasses. The contact angle was less than 10 degrees. The transparent adherent substrates would have smaller contact angle as coating time increases. After coating to a certain amounts, the degree of contact angle would not decrease. The amount of deionized water and illuminating time of UV would also affect the contact angle. The larger amount of the deionized water is, the larger the degree the contact angle is. This study used 40  $\mu$ l and 140  $\mu$ l deionized water under 20 min UV light illumination (15W, wavelength 360 nm) for contact angle measurements. The results are shown in Tables 5 and 6. The transparent TiO<sub>2</sub> thin film substrates prepared in this study had super-hydrophilic surface after illumination by UV light.

Table 5. 5% TiO<sub>2</sub> coating sol on glass.

| Coating time | Contact angle (degree) |             |
|--------------|------------------------|-------------|
|              | 40 $\mu$ l             | 140 $\mu$ l |
| 1            | 3.12                   | 5.13        |
| 2            | 2.67                   | 3.44        |
| 3            | 2.19                   | 1.98        |
| 4            | <1                     | 1.91        |
| 5            | <1                     | <1          |
| I            | 11.23                  | 16.53       |
| II           | 22.81                  | 28.14       |

I: slide glasses washed but not coating thin film.

II: slide glasses not washed and not coating thin film.

Table 6. 7% TiO<sub>2</sub> coating sol.

| Coating time | Contact angle (degree) |             |
|--------------|------------------------|-------------|
|              | 40 $\mu$ l             | 140 $\mu$ l |
| 1            | 2.37                   | 4.08        |
| 2            | 1.97                   | 2.27        |
| 3            | <1                     | <1          |
| 4            | <1                     | <1          |
| 5            | <1                     | <1          |

I: slide glasses washed but not coating thin film.

II: slide glasses not washed and not coating thin film.

## 4. Conclusion

The nanosized TiO<sub>2</sub> sol with anatase phase was successfully synthesized by hydrolysis of Ti(OH)<sub>4</sub> using HCl as the catalyst for polycondensation. The primary particles were rhombus with major axis of 20 nm and minor axis of 5 nm. It was anatase. The concentrations of acid, Ti precursor, and water could affect the formation of TiO<sub>2</sub> crystal. The higher the concentration of acid is, the higher the ratio of [H<sup>+</sup>]/[Ti] ratio is, the shorter the time needed for condensation reaction and crystal growth is. The small anatase TiO<sub>2</sub> crystal could be obtained at concentration of HCl of 1 M and [H<sup>+</sup>]/[Ti] ratio of 1.

Only a small part of the primary particles sample in 5°C aggregated into secondary particles. This is due to small kinetic energy of particles in low temperature resulting in few collisions; hence, double electric repulsive force (Stern layer and diffuse layer) is larger than van der Waals force between particles. When TiO<sub>2</sub> solid content was greater than 7% in the solution, HPC with viscosity of 150-400 cps was added to increase its stability. HPC could adsorb on TiO<sub>2</sub>

particle surface, changed its zeta potential, and avoid aggregation of particles. The TiO<sub>2</sub> thin film can be heated to 150°C to increase its surface area. The high photocatalytic activity was anticipated, because it had a large surface area of 187 cm<sup>2</sup>/g and it is microporous. The transparent TiO<sub>2</sub> thin film on substrate has super-hydrophilic property under UV light irradiation.

## Acknowledgements

This research was supported by Ministry of Science and Technology, Taiwan.

## References

- [1] Anpo M, Applications of titanium oxide photocatalysts and unique second-generation TiO<sub>2</sub> photocatalysts able to operate under visible light irradiation for the reduction of environment toxins on a global scale, *Stud Surf Sci Catal* 130: 157-166 (2000).
- [2] Bischoff BL, Anderson MA, Peptization process in the sol-gel preparation of porous anatase (TiO<sub>2</sub>), *Chem. Mater.* 7: 1772-1778 (1995).
- [3] Chrysicopoulou P, Davazoglou D, Trapalis C, Kordas G, Optical properties of very thin (<100 nm) sol-gel TiO<sub>2</sub> films, *Thin Solid Films* 323: 188-193 (1998).
- [4] Cheng H, Ma J, Zhao Z, Qi L, Hydrothermal preparation of uniform nanosize rutile and anatase particles, *Chem. Mater.* 7: 663-671 (1995).
- [5] Elfenthal L, Klein E, Rosendahl F, Process for the production of a fine particle titanium dioxide, Assignee: Kronos USA, Inc., *U. S. Patent* 5, 215, 580 (1993).
- [6] Foulger DL, Necini PG, Poeri S, Preparation of anatase titanium dioxide, Assignee: Tioxide Group Services Limited., *U. S. Patent* 5, 630, 995 (1997).
- [7] Haddow AJ, Oxidation of titanium tetrachloride to form titanium dioxide, Assignee: Tioxide Group Services Limited., *U. S. Patent* 5, 599, 519 (1997).
- [8] Kim DH, Anderson MA, Photoelectrocatalytic degradation of formic acid using a porous TiO<sub>2</sub> thin-film electrode, *Environ. Sci. Technol.* 28: 479-483 (1994).
- [9] Kostelnik RJ, Wen FC, High solids anatase TiO<sub>2</sub> slurries, Assignee: SCM Chemicals, Inc., *U. S. Patent* 5, 746, 819 (1998).
- [10] Lange RW, Sowman HG, Shaped and fired particles of TiO<sub>2</sub>, Assignee: Minnesota Mining and Manufacturing Company, *U S Patent* 4, 166, 147 (1979).
- [11] Li GL, Wang GH, Synthesis of nanometer-sized TiO<sub>2</sub> particles by a microemulsion method, *Nano Structured Mater* 11: 663-668 (1999).
- [12] Li GL, Wang GH, Synthesis and characterization of rutile TiO<sub>2</sub> nanowhiskers, *J Mater Res* 14: 3346-3354 (1999).
- [13] Mailhe-Randolph C, Mcevoy AJ, Gratzel M, Influence of precursors on the morphology and performance of TiO<sub>2</sub> photoanodes, *J Mater Sci* 26: 3305-3308 (1991).
- [14] Man HD, Lee BH, Kim SJ, Jung CH, Lee JH, Park S, Preparation of ultrafine crystalline TiO<sub>2</sub> powders from aqueous TiCl<sub>4</sub> solution by precipitation, *Japanese J App Phys* 4603-4608 (1998).
- [15] Park HK, Kim DK, Kim CH, Effect of solvent on titania particle formation and morphology in thermal hydrolysis of TiCl<sub>4</sub>, *J Am Ceram Soc* 80: 743-749 (1997).
- [16] Park SD, Cho YH, Kim WW, Kim SJ, Understanding on homogeneous spontaneous precipitation for monodispersed of TiO<sub>2</sub> ultrafine powders with rutile phase around room temperature, *J Solid State Chem* 146: 230-238 (1999).
- [17] Sakamoto M, Yokkaichi HO, Suzuka SK, Yokkaichi YY, Titania sol, Assignee: Ishihara Sangyo Kaisha, Ltd., *US Patent* 4, 880, 703 (1991).
- [18] Sato G, Arima Y, Tanaka H, Hiraoka S, Titanium dioxide sol and process for preparation thereof, Assignee: Catalyst & Chemical Industries, Co., Ltd., *US Patent* 5, 403, 513 (1995).
- [19] Sopyan L, Watanabe M, Murasawa S, Hashimoto K, Fujishima A, An efficient TiO<sub>2</sub> thin-film photocatalyst: photocatalytic properties in gas-phase acetaldehyde degradation, *J Photochem Photobio A Chem* 98: 79-86 (1996).
- [20] Takahashi H, Sakai A, Hattori M, Dendrite or asteriodal titanium dioxide micro-particles, Assignee: Ishihara Sangyo Kaisha, Ltd., *US Patent* 5, 536, 448 (1996).
- [21] Tunashima M, Muraoka K, Yamamoto K, Mikami M, Sasaki S, Stable anatase titanium dioxide and process for preparing the same, Assignee: Sakai Chemical Industry Co., Ltd., *US Patent* 6, 113, 873 (2000).
- [22] Yasumori A, Ishizu K, Hayashi S, Okada K, Preparation of a TiO<sub>2</sub> based multiple layer thin film photocatalyst, *J Mater Chem* 8: 2521-2524 (1998).
- [23] Mahshid S, Askar M, Ghamsar MS, Synthesis of TiO<sub>2</sub> nanoparticles by hydrolysis and peptization of titanium isopropoxide solution, *J Mater Processing Technol* 189: 296-300 (2007).
- [24] Oskam G, Nellore A, Penn RL, Searson PC, The growth kinetics of TiO<sub>2</sub> nanoparticles from titanium(IV) alkoxide at high water/titanium ratio, *J Phys Chem B* 107: 1734-1738 (2003).
- [25] Bui VKH, Tran VV, Moon JY, Park D, Lee YC, Titanium dioxide microscale and macroscale structures: a mini-review, *Nanomater* 10: 1190-1221 (2020).
- [26] Zhou W, Sun F, Pan K, Tian G, Jiang B, Ren Z, Tian C, Fu H, Well-ordered large-pore mesoporous anatase TiO<sub>2</sub> with remarkably high thermal stability and improved crystallinity: Preparation, characterization, and photocatalytic performance. *Adv Funct Mater* 21: 1922-1930 (2011).
- [27] Rajaraman TS, Parikh SP, Gandhi VG, Black TiO<sub>2</sub>: A review of its properties and conflicting trends, *Chem Eng J* 389: 123918-123929 (2019).
- [28] Yoshihisa O, Kazuhito H, Fujishima A, Kinetic of photocatalytic reactions under extremely low-intensity UV illumination on titanium dioxide thin film, *J Phys Chem A* 101: 8057-8062 (1997).
- [29] Zhang Q, Gao L, Guo J, Effects of calcinations on the photocatalytic properties of nanosized TiO<sub>2</sub> powders prepared by TiCl<sub>4</sub> hydrolysis, *Appl Catal B Environ* 26: 207-215 (2000).

- [30] Zeng TY, Qiu Y, Chen LH, Song X, Microstructure and phase evolution of TiO<sub>2</sub> precursors prepared by peptization-hydrolysis method using polycarboxylic acid as peptizing agent, *Mater Chem Phys* 56: 163-170 (1998).
- [31] Zima YM, Karakchiev LG, Lyakhov NZ, Synthesis and physicochemical properties of hydrated titanium dioxide sol, *Colloid J* 4: 471-475 (1998).
- [32] Eremenko BV, Bezuglaya TN, Savitskaya AN, Malysheva ML, Kozlov IS, Bogodist LG, Stability of aqueous dispersions of the hydrated titanium dioxide prepared by titanium tetrachloride hydrolysis, *Colloid J* 63: 173-178 (2001).
- [33] Ravishankar TN, Vaz MO, Teixeira SR, The effects of surfactant in the sol-gel synthesis of CuO/TiO<sub>2</sub> nanocomposites on its photocatalytic activities under UV-visible and visible light illuminations, *New J Chem* 44: 1888-1904 (2020).